

## Thermochromism of Merocyanine J-Aggregate Monolayers on Binary Counterion Subphases

Noritaka Kato, Yuji Ikegami, Yoshiaki Uesu,

Department of Physics, Waseda University, Tokyo 169-8555, Japan

Fax: +81-3-5286-3446, e-mail: n.k@waseda.jp

The thermochromism of the merocyanine J-aggregates was investigated using the binary counterion subphase containing  $Mg^{2+}$  and  $Sr^{2+}$  ( $Mg^{2+}/Sr^{2+}$  subphase). The behaviors of the thermochromic transition on the  $Mg^{2+}/Sr^{2+}$  subphase and that on the subphase containing  $Mg^{2+}$  and  $Cd^{2+}$  were compared, and the difference was discussed from the viewpoint of the hydrated ionic radii of the counterions.

Key words: Thermochromism, J-aggregates, Langmuir films

### 1. INTRODUCTION

A J-aggregate [1] is an assembly of organic dye molecules, and is characterized by a sharp, intense and red-shifted visible absorption band (J-band) compared to that of monomeric dye molecules. In a dye aggregate having an ordered molecular arrangement, the transition dipole interaction among the dye molecules splits the degenerated states of the molecules, resulting in a formation of a band structure. Dye aggregates, whose optically allowed transition levels are the lowest energy ones in their bands, are classified in the J-aggregates. Such aggregates are useful for the optical sensitizing in conventional photography [2,3] and candidates for ultra-fast nonlinear optical devices [4].

An amphiphilic merocyanine dye (MD) molecule that has an electric dipole moment in its chromophore (Fig. 1) forms two-dimensional J-aggregates on an aqueous subphase [5,6], and the MD J-aggregates exhibit a pronounced J-band, whose energy level depends on the conditions of the subphase [7,8]. A recent X-ray structural analysis and a theoretical consideration on the MD J-aggregate monolayer revealed that not only the transition dipole interaction but also the electric dipole interaction among the MD molecules contributed to the energy shift of the absorption band upon aggregation [9].

The MD J-aggregate shows a thermochromic phase transition on the subphase containing two kinds of counterions (binary counterion subphase) [10,11]. A switching of the J-band wavelength between 595 and 620 nm occurs at certain subphase temperatures and the J-band wavelength exhibits a thermal hysteresis loop. So far, we had investigated the phase transition using the binary counterion subphases containing a pair of  $Mg^{2+}$  and  $Cd^{2+}$  ( $Mg^{2+}/Cd^{2+}$  subphase) [10,11] or a pair of  $Zn^{2+}$  and  $Cd^{2+}$  ( $Zn^{2+}/Cd^{2+}$  subphase) [12]. On the  $Mg^{2+}/Cd^{2+}$  subphase, it had been shown that the molecular arrangement in the aggregate of the J-band at 595 nm was different form that in the aggregate of the J-band at 620 nm by grazing incidence X-ray diffraction measurements [13]. Therefore, the thermochromism is the structural phase transition in the MD J-aggregate. Also, it had been found that the thermochromic behaviors observed on the  $Mg^{2+}/Cd^{2+}$  subphase and the  $Zn^{2+}/Cd^{2+}$  subphase were more or less similar, and it had

been considered that this similarity might be attributed to almost the same hydrated ionic radii between  $Mg^{2+}$  and  $Zn^{2+}$  [12]. This consideration implies that the hydrated ionic radius of the counterion is a key factor to understand not only the formation of the MD J-aggregate but also the mechanism of the thermochromic phase transition in the MD J-aggregates.

For a further investigation of the ionic radius dependence of the thermochromic behavior,  $Sr^{2+}$  ion, whose hydrated ionic radius is larger than the radii of  $Mg^{2+}$  and  $Cd^{2+}$  ions, is employed for one of the binary counterions, and the thermochromism observed on the binary counterion subphase containing  $Mg^{2+}$  and  $Sr^{2+}$  ( $Mg^{2+}/Sr^{2+}$  subphase) is reported.

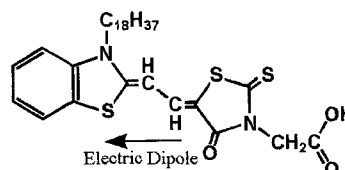


Fig. 1 Molecular structure of amphiphilic merocyanine dye molecule.

### 2. EXPERIMENTAL

A powder of the MD molecules was purchased from Hayashibara Biochemical Laboratory, Inc., and a chloroform solution of MD (1 mM) was prepared as a spreading solution. For the counterions,  $MgCl_2$  and  $SrCl_2$  were obtained from Kanto Chemical Co., Inc. Pure water for the subphases was prepared in a Milli-Q system, and its resistivity was greater than 18  $M\Omega$  cm. Aqueous solutions of  $MgCl_2$  and  $SrCl_2$  were used for the binary counterion subphases. The total concentration of the chlorides was fixed at 0.5 mM =  $[MgCl_2] + [SrCl_2]$ , and the molar ratio  $\rho = [SrCl_2]/([MgCl_2] + [SrCl_2])$  was varied between 0 and 100%. To keep the pH value of the subphases around 7,  $NaHCO_3$  was added up to 0.06 mM. After spreading the MD molecules on these subphases, the J-aggregates were formed immediately without any compression of the MD monolayer.

A trough without a barrier and a pressure sensor was made according to the literature [14]. Underneath the trough, eight Peltier devices were equipped. A Peltier controller (Cell System Co., LTD) was connected

between a DC power source (PAN 110-10A, Kikusui Electronics Corp.) and the Peltier devices to control the subphase temperature from 0 to 40 °C at an accuracy within  $\pm 0.3$  °C. The trough was placed in a chamber and the chamber was purged with N<sub>2</sub> gas at  $0.3 \pm 0.1$  L/min to prevent a bleach of the MD molecules due to the oxidation. The spreading amount of the MD molecules was regulated to be sure that the surface pressure was below 0.5 mN/m. The subphase temperature was changed step by step. Incubation was performed for at least 15 min after each temperature change, followed by the reflectance measurement.

Because the absorption and the reflection spectra showed almost the same peak wavelength [10,11] and the optical setup of the reflection geometry was simpler than the transmission type, the J-band was monitored by reflection spectroscopy. A bundle of two optical fibers was introduced into the trough chamber and placed above the monolayer. One fiber illuminated the monolayer with white light and the other one transferred the vertically reflected light to the spectrometer (EPP2000, StellarNet Inc.), having a resolution of 0.7 nm.

### 3. RESULTS AND DISCUSSION

The J-band wavelength of the monolayer on the Mg<sup>2+</sup>/Sr<sup>2+</sup> subphase was investigated with varying the  $\rho$  value at a fixed subphase temperature of 25 °C. At each  $\rho$  value, the monolayer was formed and the J-band wavelength was observed (Fig. 2). At  $\rho = 0\%$ , the J-band wavelength was located at 620 nm, and the spectrum is shown in the inset of Fig. 2. The J-band wavelength was located between 620 and 621 nm up to  $\rho = 55\%$ . At  $\rho = 60\%$ , the J-band wavelength was observed at 610.5 nm and stayed at almost the same wavelength up to  $\rho = 100\%$ . The wavelength was 610.5 nm at  $\rho = 100\%$ . The spectrum observed at  $\rho = 100\%$  is shown in the inset of Fig. 2. The large shoulder on a shorter wavelength side of the 610.5 nm J-band is a characteristic of this J-aggregate, suggesting that its molecular arrangement is different from the J-aggregates formed by Mg<sup>2+</sup> or Cd<sup>2+</sup>, and the reflection intensity of the J-band at 611 nm was less than 20% of the intensity of the J-band at 620 nm.

According to the discreet change in the J-band wavelength shown in Fig. 2, it can be judged that a boundary between the phase of the J-band at ca. 611 nm (J611) and that of the J-band at ca. 620 nm (J620) locates around  $\rho = 57.5\%$ .

In Fig. 3, the J-band spectra observed at different temperatures on the Mg<sup>2+</sup>/Sr<sup>2+</sup> subphase at  $\rho = 0\%$  are shown. The MD monolayer was formed at a subphase temperature of 33.0 °C, and the spectrum was obtained by decreasing the temperature step by step. At 33.0 °C, the J-band peak was located at 620.5 nm, and this corresponds to the phase of J620 (Fig. 2 inset). On cooling, the J-band wavelength exhibited a slight shift, and was observed at 619.5 nm at 9.0 °C. When the temperature was decreased from 9.0 °C to 7.0 °C, the discreet shift of the J-band wavelength from 619.5 to 612.5 nm occurred, and the peak wavelength did not change down to 2.5 °C. As shown in Fig. 3, the spectrum at 7.0 °C has higher reflectance than that at 5.5 °C on the longer wavelength side of the peak, indicating that the aggregate of J-band at ca. 612 nm coexisted with the

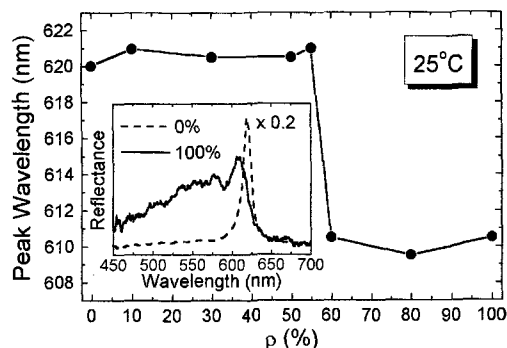


Fig. 2 Dependence of the J-band wavelength on the molar ratio of counterions  $\rho$  at the subphase temperature of 25 °C. The inset indicates the reflection spectra of the monolayers at  $\rho = 0\%$  and 100%. The former intensity was multiplied by 0.2 to have a comparable intensity to the latter.

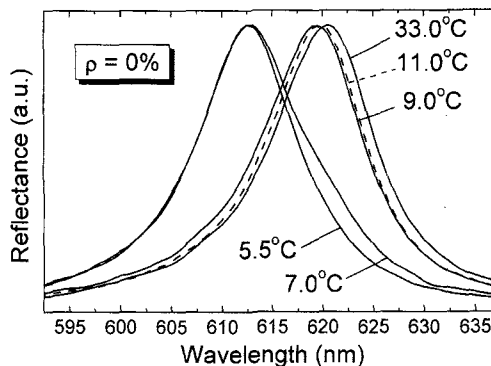


Fig. 3 Normalized J-band spectra of the monolayer on the Mg<sup>2+</sup>/Sr<sup>2+</sup> subphase of  $\rho = 0\%$ . The observation was performed on cooling.

phase of J620 at 7.0 °C. Although the peak wavelength of the phase of J611 is close to 612 nm, the spectral shape of the J-band at ca. 612 nm in Fig. 3 is obviously different from that of the phase of J611 (the inset in Fig. 2). Therefore the aggregate of J-band at ca. 612 nm in Fig. 3 should be assigned to another phase of J612.

After the cooling process (Fig. 3), the heating process was carried out. The J-band at 612.5 nm was shifted back to 619.5 nm when the temperature was increased from 8.5 °C to 11.5 °C, and a further increase in the temperature to 33.0 °C induced a slight shift from 619.5 to the initial wavelength of 620.5 nm. These temperature dependences of the J-band wavelength on cooling and heating are summarized in Fig. 4(a) as a thermal hysteresis loop of the peak wavelength. For simplicity, the plotted wavelengths are the peak wavelengths of the spectra even if the different phases coexisted. Fig. 4(a) clearly shows that the reversible thermochromic phase transition between the phases of J620 and J612.

The temperature dependences of the J-band wavelength were also investigated using the Mg<sup>2+</sup>/Sr<sup>2+</sup> subphases of  $\rho = 10\%$ , 30%, and 50%, and the obtained thermal hysteresis loops are indicated in Fig. 4(b), (c), and (d), respectively. All of them show the phase of J612 as a low temperature phase and the phase of J620 as a high temperature phase. The shapes of the loops are more or less the same, but the width of the hysteresis

increases as the  $\rho$  value increases.

When the  $\text{Mg}^{2+}/\text{Sr}^{2+}$  subphases of  $\rho = 60\%$  was used, the thermochromic behavior was changed drastically. When the monolayer was formed on the  $\text{Mg}^{2+}/\text{Sr}^{2+}$  subphases of  $\rho = 60\%$  at  $35.5^\circ\text{C}$ , the J-band wavelength was observed at  $609.5\text{ nm}$  and the spectral shape indicated that the phase corresponded to J611. On cooling, the J-band wavelength showed no particular temperature dependence. The peak wavelength was located around  $611\text{ nm}$  as shown in Fig. 5(a), and the reflection spectra at three different temperatures are shown in Fig. 6. It is clear that the spectrum of the phase of J611 does not show any temperature dependence. As on cooling, no temperature dependence of the J-band

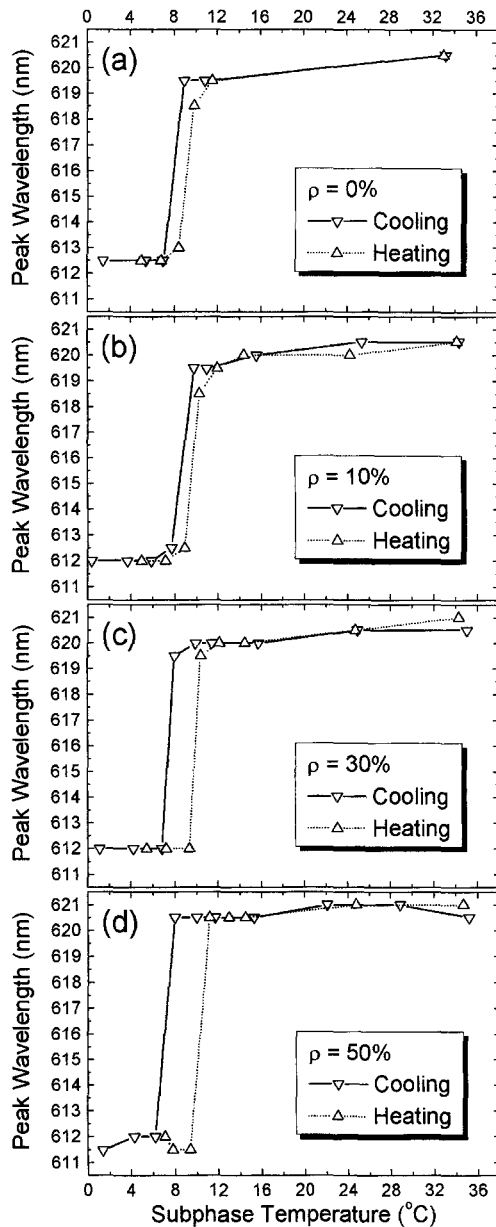


Fig. 4 Thermal hysteresis loops of the J-band wavelength observed on the  $\text{Mg}^{2+}/\text{Sr}^{2+}$  subphases of (a)  $\rho = 0\%$ , (b)  $10\%$ , (c)  $30\%$ , and (d)  $50\%$ . The cooling process was followed by the heating process for all conditions.

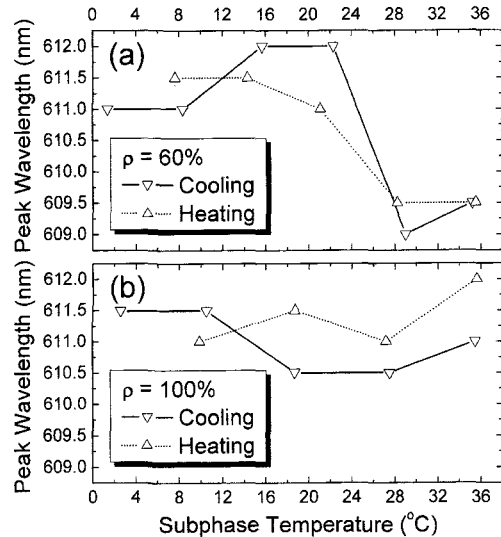


Fig. 5 Temperature dependence of the J-band wavelength observed on the  $\text{Mg}^{2+}/\text{Sr}^{2+}$  subphases of  $\rho = 60\%$  and  $100\%$ . The cooling process was followed by the heating process for both conditions.

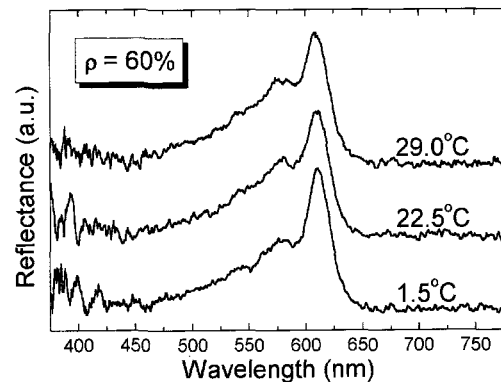


Fig. 6 Reflection spectra of the monolayer on the  $\text{Mg}^{2+}/\text{Sr}^{2+}$  subphase of  $\rho = 60\%$  at three different temperatures. The spectra were offset for easier viewing.

wavelength was observed on heating as shown in Fig. 5(a). On the  $\text{Mg}^{2+}/\text{Sr}^{2+}$  subphase of  $\rho = 80\%$  and  $100\%$ , the phase of J611 was also formed at ca.  $36^\circ\text{C}$  after spreading the MD molecules, and the J-band wavelength stayed around  $611\text{ nm}$  on cooling and heating. Fig. 5(b) shows the result obtained at  $\rho = 100\%$ . Therefore, it is concluded that, above  $\rho = 60\%$ , there is only one phase of J611 in the range of the subphase temperature below  $35.5^\circ\text{C}$ .

According to the obtained temperature dependences of the J-band wavelength in Figs. 4 and 5 as well as the  $\rho$  dependence of the J-band wavelength at  $25.0^\circ\text{C}$  in Fig. 2, the phase diagram of the  $\rho$  value versus the subphase temperature can be drawn as shown in Fig. 7. From Fig. 4, between  $\rho = 0\%$  and  $50\%$ , there are two phases of J620 and J612 that show the thermal hysteresis around  $8^\circ\text{C}$ . Above  $\rho = 60\%$ , there is only one phase of J611. From the result shown in Fig. 2, the boundary of the two-phase region of J620 and J612 and the one-phase region of J611 should be located around  $\rho = 57.5\%$ .

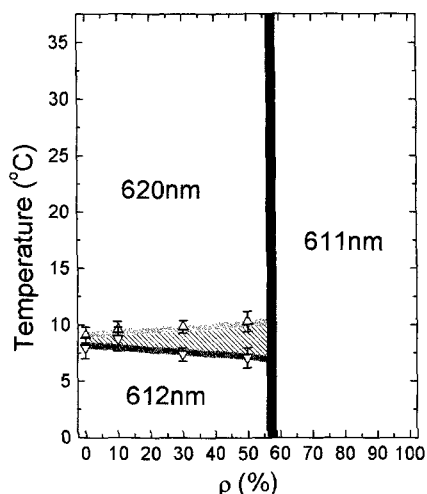


Fig. 7 Phase diagram of the subphase temperature versus the molar ratio of counterions  $\rho$ . The plots are the phase transition temperatures determined from the hysteresis loops shown in Fig. 4, and the shaded region corresponds to the width of the hysteresis loops. The dark gray line indicates the phase transition temperature on cooling and the bright gray line on heating.

The phase diagrams obtained using the  $\text{Mg}^{2+}/\text{Sr}^{2+}$  and  $\text{Mg}^{2+}/\text{Cd}^{2+}$  subphases are quite different from each other [10,11]. The latter also induces three phases. Two of them correspond to J620 and J612, and the other phase exhibits the J-band at 595 nm (J595) [12]. The  $\text{Mg}^{2+}/\text{Cd}^{2+}$  subphase induces the thermochromic phase transition among the three phases and the phase transition temperatures depend on the  $\rho$  value [12]. On the other hand, the  $\text{Mg}^{2+}/\text{Sr}^{2+}$  subphase induces the thermochromic phase transition only between the phases of J620 and J612 with a small dependence of the phase transition temperatures on the  $\rho$  value, and the phase of J611 exhibits no thermochromic phase transition (Fig. 7). The only difference between the  $\text{Mg}^{2+}/\text{Sr}^{2+}$  and  $\text{Mg}^{2+}/\text{Cd}^{2+}$  subphases is the species of one of the counterions. Therefore, the difference in the thermochromic behavior between these subphases should be attributed to the size difference between  $\text{Sr}^{2+}$  and  $\text{Cd}^{2+}$  ions, which have the hydrated ionic radii of ca. 263 pm and 230 pm, respectively [15].

#### 4. CONCLUSIONS

The thermochromic behavior was investigated using the  $\text{Mg}^{2+}/\text{Sr}^{2+}$  subphase, and was summarized in the phase diagram of the subphase temperature versus the  $\rho$  value (Fig. 7). The three phases of J620, J612 and J611 were induced on the subphase. The phases of J620 and J611 exhibited the sharp and intense reflectance at their J-band wavelengths. The phase of J611 showed the weak reflection intensity at the peak with the large and broad shoulder on the shorter wavelength side of the peak, and this J-aggregate state was different from those observed on the  $\text{Mg}^{2+}/\text{Cd}^{2+}$  subphase. The thermochromic phase transition occurred only between the phase of J620 and J612, and the phase of J611 did not show the thermochromism. This thermochromic behavior is different from that observed on the

$\text{Mg}^{2+}/\text{Cd}^{2+}$  subphase. These results indicate that the difference in the hydrated ionic radius affects not only the J-aggregate formation of MD molecules but also the thermochromic behavior of the MD J-aggregates on the binary counterion subphase.

#### 5. ACKNOWLEDGMENTS

This work was supported by the Saneyoshi Scholarship Foundation and Grant-in-Aids for Young Scientists (B) 17760015, 2005 and The 21st Century COE Program (Physics of Self-Organization Systems) at Waseda University from MEXT, Japan.

#### References

- [1] T. Kobayashi (Ed.), "J-Aggregates", World Scientific, Singapore (1996).
- [2] A. H. Herz, *Photogr. Sci. Eng.* **18**, 323 (1974).
- [3] T. Tani, *J. Disp. Sci. Technol.*, **25**, 375 (2004).
- [4] M. Furuki, M. Tian, Y. Sato, L. S. Pu, S. Tatsuura, and O. Wada, *Appl. Phys. Lett.*, **77** 472 (2000).
- [5] M. Sugi, T. Fukui, S. Iizima and K. Iriyama *Mol. Cryst. Liq. Cryst.* **62**, 165 (1980).
- [6] K. Iriyama, M. Yoshimura, Y. Ozaki, T. Ishii, S. Yasui, *Thin Solid Films* **132**, 229 (1985).
- [7] M. Yoneyama, T. Nagano, T. Murayama, *Chem. Lett.*, 397 (1989).
- [8] T. Kawaguchi, K. Iwata, *Thin Solid Films* **191**, 173 (1990).
- [9] N. Kato, K. Yuasa, T. Araki, I. Hirose, M. Sato, N. Ikeda, K. Iimura, Y. Uesu, *Phys. Rev. Lett.* **94**, 136404 (2005).
- [10] N. Kato, K. Saito, T. Serata, H. Aida, Y. Uesu, *J. Chem. Phys.* **115**, 1473 (2001).
- [11] N. Kato, K. Saito, T. Serata, H. Aida, and Y. Uesu, "Ferroelectrics Vol. 2", edited by V. Stefan, The Stefan University Press Series on Frontiers in Science and Technology, La Jolla, CA (2002), pp81–110.
- [12] N. Kato, T. Araki, Y. Uesu, *Colloids Surf. A. Physicochem. Eng. Aspects*, in press.
- [13] N. Kato, T. Araki, Y. Uesu, I. Hirose, N. Ikeda, K. Iimura, *Ferroelectrics* **314**, 135 (2005).
- [14] T. Kato, A. Tatehana, N. Suzuki, K. Iimura, K. Iriyama, *Jpn. J. Appl. Phys.* **34**, L911 (1995).
- [15] H. Ohtaki, T. Radani, *Chem. Rev.* **93**, 1157 (1993).

(Received December 11, 2005; Accepted January 19, 2006)